

# Data-driven Model Predictive Control for Power Demand Management and Fast Demand Response of Commercial Buildings using Support Vector Regression

Rui Tang<sup>1</sup>, Cheng Fan<sup>2,\*</sup>, Fanzhe Zeng<sup>3</sup> and Wei Feng<sup>4</sup>

<sup>1</sup> Institute for Environmental Design and Engineering, University College London, London, UK

<sup>2</sup> Sino-Australia Joint Research Center in BIM and Smart Construction, College of Civil and Transportation Engineering, Shenzhen University, Shenzhen, China

<sup>3</sup> School of Municipal and Environmental Engineering, Shenyang Jianzhu University, Shenyang, China

<sup>4</sup> China Energy Group, Lawrence Berkeley National Laboratory, Berkeley, CA, USA

**Abstract:** Demand response (DR) of commercial buildings by directly shutting down part of operating chillers could provide an immediate power reduction for power grids. In this special fast DR event, effective control needs to guarantee expected power reduction and ensure an acceptable indoor environment. This study, therefore, developed a data-driven model predictive control (MPC) using Support Vector Regression (SVR) for fast DR events. According to the characteristics of fast DR events, the optimized hyperparameters of SVR and shortened searching range of genetic algorithm are used to improve the control performance. Meanwhile, a comprehensive comparison with RC-based MPC is conducted based on three scenarios of power demand controls. Test results show that the proposed SVR-based MPC could fulfill the control objectives of power demand and indoor temperature simultaneously. Compared with RC-based MPC, the SVR-based MPC could alleviate the time/labor cost of model development without sacrificing the control performance of fast DR events.

**Keywords:** demand response; support vector regression; machine learning; building peak demand; model predictive control; smart grid.

## 1. Introduction

The increasing demand for electricity and the rapid development of renewable energy systems that is difficult to be accurately predicted due to uncertain weather conditions are challenging the reliable operation of power grids (Tuballa & Abundo, 2016). Keeping the real-time balance of power grids between supply and demand sides is a critical issue. Peak demand is one big concern to induce power imbalance by challenging the capacity limit of power supply. A huge expense is spent to upgrade the capacity of power grids to overcome the problem of peak demand. The capacity for the top 100 hours peak demand in a year accounts for nearly 20% of electricity costs of power grids. Due to the infrequent occurrence of these peaks, this part of the grid capacity associated with transmission and generation is however wasted most of the time in a year (Arnold, 2011). Demand response (DR) is considered a promising solution to help power grids operate more smartly by enhancing reliability, security, and flexibility. DR programs encourage end-users (i.e., demand side of power grids) to address the power imbalance using pricing information or economic incentives. The end-users adjust their power utilization responding to the needs of power grids. DR programs can benefit power grids by avoiding the huge cost and ensuring healthy operation, and meanwhile, building owners obtaining the economic benefits (Tang et al., 2019).

### *Building demand response towards smart grids*

Among power consumers at the demand side of power grids, the building sector consumes about 40% of global energy used (Kolokotsa et al., 2011). This share is still increasing as the rapid growth of population, living quality improvement, urbanization, etc. Building accounted for 74% of electricity use in the United States in 2010 (U.S. Department of Energy, 2011) and 90% of total electric energy in Hong Kong in 2012 (EMSD of Hong Kong, 2014). The power use in buildings has elastic characteristics and hence feasible to alter their loads for power demand-side management. In commercial buildings, heating, ventilation, and air-conditioning (HVAC) systems, accounting for more than 50% of energy consumption, are preferable to be used as a DR resource (Tang et al., 2018). Meanwhile, building automation systems and advanced technologies such as smart meters (Depuru et

al., 2011) could benefit the implementation of DR controls. Demand shifting and demand limiting are two main methods for building DR controls. Demand shifting by rescheduling the operation of central air-conditioning systems is widely adopted, which part of peak load (with high price) is shifted to non-peak periods (with low price). Demand limiting is to reduce and even switch off the non-essential electric load in peak demand or DR events.

Indoor air temperature reset strategy is a popular way to reshape the building power utilization for DR events (Motegi et al., 2007; Yin et al., 2010). But the key shortage of this method is the response time. By resetting indoor air temperature, building power demand cannot be changed immediately within a very short period, responding to urgent needs/requests (e.g., sudden price change) of power grids. This is because of the inherent delay in the system reaction after the set-point changes of control states. To provide an immediate power reduction in commercial buildings, limiting the load of operating chillers attracted extensive attention. Chillers account for high power demand (even more than half in some cases) in cooling systems of commercial buildings (Pérez-Lombard et al., 2008). Shutting down parts of operating chillers is therefore regarded as an effective fast DR control strategy and many related studies have been conducted recently. Xue et al. (2015) conducted a simulation test to validate the reaction delay of indoor temperature reset strategies and discussed the necessity of fast demand response. Tang et al. (2016) pointed out that without proper control after switching off part of operating chillers, system power demand could not be reduced effectively. Under limited cooling supply, the pumps and fans would be fully operated, and hence increased system power demand and reduced the effect of DR controls. This was because the current existing control strategies in central air-conditioning systems were useful on the premise of an assumption of sufficient cooling provided by chillers. To solve the control failure problem under limited operating chillers, a supply-based control strategy (Wang & Tang, 2017) was developed for proper cooling distribution among individual zones. Cui et al. (2015) developed an optimal control strategy to manage the power demand of a central air-conditioning system integrated with small-scale thermal storage under a limited number of operating chillers. Ran et al. (2020) developed a virtual sensor-based self-adjusting control strategy during fast DR events to optimize the chilled water flow of each AHU (air handling unit) for expected indoor

temperature control.

### Model predictive control for building demand response

Model predictive control (MPC) is an advanced method of processing control that is used to control a process while satisfying a set of constraints (Morari & Lee, 1999). Due to its advantages of control robustness and accuracy (Afram & Janabi-Sharifi, 2014), many studies are conducted on the applications of MPC for building power demand management and DR controls (Avcı et al., 2013; Huang et al., 2009; Oldewurtel et al., 2012; Zong et al., 2012). Killian and Kozek (2016) summarized ten questions concerning MPC for energy-efficient buildings, spanning from the benefits of MPC, how to set up the MPC framework, and challenges of MPC implementation in real buildings to future direction of integrating MPC-based building control into smart grids and renewable energy resources. Olivieri et al. (2013) developed MPC-based optimal control strategies to achieve the building power demand reduction as utility needed. Three variables in the cooling system were optimized by MPC, i.e., return air temperature, chilled water temperature, and supply air temperature. Mai and Chung (2014) formulated a robust MPC algorithm to manage the power demand of HVAC systems in group-level commercial buildings.

The core of MPC is to develop a model to grasp the building system dynamics. Compared with the models in building simulation software, RC (resistance–capacity) physical-based models based on the energy conservation law could be developed without rather detailed parameters that are costly and impractical to be collected from a real project. But considerable expert knowledge and engineering experience and information such as weather information, internal heat gain, and building geometry are still required. Also, a specific developed RC model is not scalable and fit for other buildings. RC models are therefore challenged by the time-consuming and labor-intensive although it is widely adopted for MPC in building system controls. As the technology of machine learning emerging, data-driven models elicit much attention in building energy modeling (Fan et al., 2021), which own flexible structures for possibly extendable to different buildings. Data-driven models could save the efforts and time required for physical-based models by directly analyzing data inputs and outputs to

comprehensively identify the interactions of different variables. SVR (support vector regression) is a widely used data-driven approach to predict the building energy dynamics due to its strong capability of non-linear and time-series predictions. SVR transforms the nonlinear problems as linear by mapping input and output data into a high-dimensional feature space for the enhancement of prediction accuracy and robustness. Chen et al. (2017) developed an SVR model to predict the short-term electrical load of office buildings as the baseline of demand response. Zhang et al. (2016) proposed a time-series forecasting strategy for the prediction of building energy consumption using SVR. Paniagua-Tineo et al. (2011) predicted daily maximum temperature using SVR and prediction results outperformed neural networks. Pourjafari and Reformat (2019) proposed an SVR-based MPC for the volt–var optimization of electrical distribution systems. Xi et al. (2007) developed an SVR-based MPC for simultaneous and accurate control of temperature and relative humidity served by a central air-conditioning system. The control performance was better than the results when using neural fuzzy control. Generally, SVR is widely applied for building load prediction, but limited studies were conducted to combine SVR with MPC for building thermal system control, which has been commonly used in other domains such as electrical engineering.

When applying data-driven methods in MPC, the key question is how to find the optimum due to the nonlinear characteristics of data-driven models. The optimization method for data-driven MPC can be categorized into dynamic programming, gradient-based method, and intelligent algorithm (Wang et al., 2019). Dynamic programming can find the optimal solution by converting the data-driven model into a convex optimization problem. This method requires proficient knowledge of machine learning to transform nonlinear and nonconvex problems into convex optimization (Smarra et al., 2018). Moreover, the efforts and time costs are therefore shifted from RC model development to the processing of complicated optimization problems. Gradient-based methods, as numerical solutions, can achieve a fast convergence but are sensitive to the initial value of control variables, which increases the risks of local convergency and meaningless results. Compared with the numerical solutions, intelligent algorithms are less sensitive to the initialization and less troubled by local optimum, but the computational efficiency is lower.

### Research gap and objectives

During fast DR events, few studies are conducted in the literature to optimize the system operation using data-driven MPC. Additionally, limiting chiller power demand in buildings would be applicable in other conditions such as the cooling systems are operating abnormally, not only limited to fast DR events. Recently more renewable energy resources are trying to be integrated into building energy systems, which potentially increases the need for building energy flexibility. Li and Peng et al. (2020) studied the dynamic energy matching performance between photovoltaic generation and load of PV direct-driven air conditioning systems at minute-level time scale to improve the evaluation in a transient way. From the perspective of system resilience, the advanced control strategy can effectively relieve the negative influences on the indoor environment under the limited cooling supply and hence guarantee a good control performance. This study, therefore, intends to bridge the gap of how to apply the data-driven MPC for fast demand response control. The proposed MPC aims to achieve an expected power demand control and create the best possible indoor environment simultaneously in fast DR events. Genetic algorithm (GA) is adopted for online optimization considering the computational speed. The main contributions of this study include:

(1) Data-driven MPC based on the SVR prediction model is applied for fast DR periods and its control performance is validated by comparing with the RC-based MPC; (2) Searching range of GA for online optimization is narrowed down fully taking the characteristics of fast DR event into account to alleviate the local convergence and increase the computational speed. The penalty function is applied to address the constraints of indoor temperature when setting the objective function of GA optimization; (3) Three scenarios of control objectives in fast DR events, i.e., minimum and smooth power demand, maximum and smooth power demand reduction, and maximum average power demand reduction, are studied to satisfy different DR programs and also validate the control performance of proposed control strategy under different conditions.

## **2. Schematic of MPC-based building power demand control in DR events**

Fig.1 illustrates the schematic of chiller power demand control in a fast DR event. Once an urgent

request from power grids, the DR control is activated by switching off part of operating chillers directly for an immediate power reduction within a very short time. Three modules (i.e., chiller power demand optimizer, chiller load regulator, and cooling distributor) are responsible to ensure the DR control implemented properly to maximize revenues/rewards obtained from power grids and keep the indoor environment acceptable. The *chiller demand optimizer* is to optimize the chiller power demand set-points considering the control objectives and constraints (e.g., indoor environment). The function of this module is realized by the MPC approach. The *chiller load regulator* is to implement the optimized set-point of chiller power demand online by adjusting the total chilled water flow into the buildings using the PID algorithm amplified by a factor  $K$ . Under the total cooling supply adjusted by the chiller load regulator represented by the chilled water flow of the secondary loop, the *cooling distributor* is responsible for allocating the cooling supply properly among individual AHUs. This study is focused on developing the module of *chiller demand optimizer* using data-driven model predictive control (MPC) and the works for the modules of *chiller load regulator* (Tang et al., 2018) and *cooling distributor* (Tang et al., 2016) can be found in the previous studies.

In this study, the indoor environment is described by indoor temperature, which has the highest impact on the indoor environment compared with other factors (e.g., relative humidity). The immediate power reduction during DR events is contributed by chillers in a central air-conditioning system.

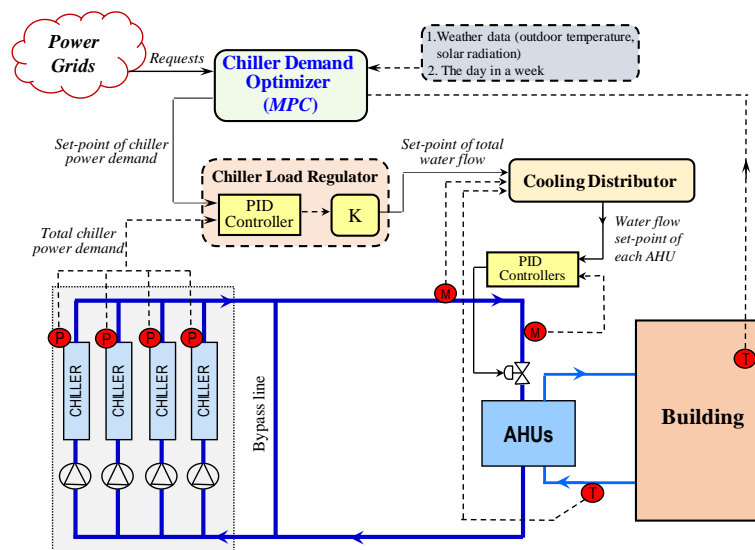


Fig.1 Schematic of chiller power demand control during fast DR events

### 3. Data-driven MPC for chiller demand optimizer in DR controls

#### 3.1 Principle of MPC for chiller demand optimizer

Fig.2 presents the principle of MPC in the system real-time (online) optimal control in fast DR events. The MPC framework developed includes three parts, i.e., dynamic model (SVR-based model, section 3.2), model correction (section 3.3), and (online) optimization (section 3.4). At a sampling interval, MPC optimizes the current timestep while keeping the future into account. Based on the collected information (weather data, the trajectory of chiller power demand set-point, etc.), the dynamic model predicts system responses of targeted states ( $y'$ , predicted indoor temperature in this study) under a given group of control state values over the prediction horizon. The modification/correction using a factor ( $e$ ) is to effectively address the disturbances and unpredictable errors for improving the prediction accuracy and control performance based on the measured indoor temperature ( $y$ ). The optimization result of chiller power demand set-point is a trajectory of future control signals that satisfy the system dynamics and the corresponding constraints. But only the first control signal ( $u$ , chiller power demand set-point) is sent to the system for implementation at the next sampling time and the rest of the sequence is discarded. This process is repeatedly implemented at the following process using the updated states of the next prediction horizon.

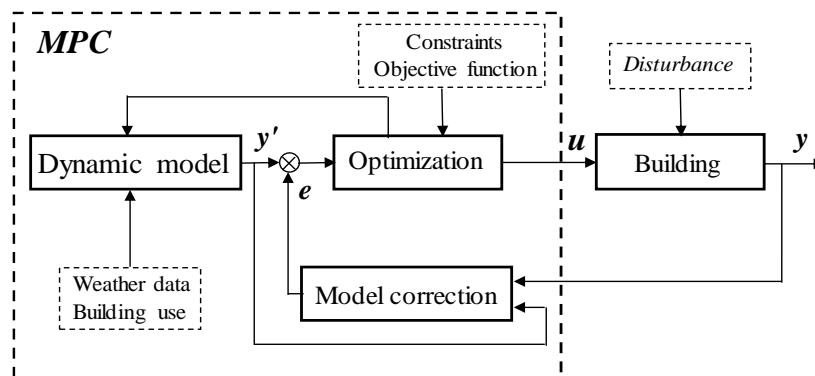


Fig.2 Principle of MPC strategy for chiller demand optimizer during fast DR events

#### 3.2 Development of dynamic models for MPC

##### 3.2.1 SVR model

- Principle of SVR

SVR (support vector regression) is a promising machine learning approach for data regression because of its powerful capability for nonlinear predictions (Ahmad et al., 2018). The regression function of SVR is shown in Eq.(1). Where  $f(\mathbf{x})$  is the prediction value.  $\mathbf{W}$  is the high-dimensional weight factor.  $b$  is an adjustable factor.  $\varphi(\mathbf{x})$  represents the mapping function.  $\mathbf{x}$  is the inputs.

$$f(\mathbf{x}) = \mathbf{W}^T \varphi(\mathbf{x}) + b \quad (1)$$

The residual value between prediction  $f(\mathbf{x})$  and actual value  $y$  is defined as Eq.(2). The ideal regression model is set as the full residual within a range of  $\varepsilon$ , as shown in Eq.(3). The distances between data outside of the tube and identified hyperplane are  $\xi$  (larger than  $\varepsilon$ ) and  $\xi^*$  (lower than  $-\varepsilon$ ). Fig.3 illustrates the schematic of key parameters ( $\pm\varepsilon$ ,  $\xi$ , and  $\xi^*$ ) and identified hyperplane in the SVR approach.

$$R(x, y) = y - f(\mathbf{x}) \quad (2)$$

$$-\varepsilon \leq R(x, y) \leq \varepsilon \quad (3)$$

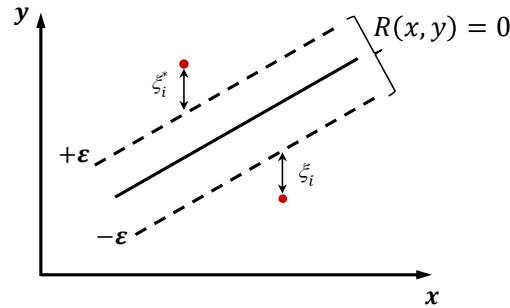


Fig.3 Schematic of Support Vector Regression

The SVR identifies the optimum hyperplane by making the hyperplane maximum flat (first term of Eq.(4)) and addressing the data outside the tube with a penalty (second term of Eq.(4)). Where  $C$  is a penalty factor to determine the trade-off between training error and model flatness. The SVR optimization objective is subject to the constraints in Eqs.(5-7).

$$\min F(\mathbf{W}, b, \xi_i, \xi_i^*) = \frac{1}{2} \|\mathbf{W}\|^2 + C \sum_{i=1}^N (\xi_i + \xi_i^*) \quad (4)$$

*Subject to:*

$$y_i - \mathbf{W}^T \varphi(\mathbf{x}_i) - b \leq \varepsilon + \xi_i \quad i = 1, 2, \dots, N \quad (5)$$

$$\mathbf{W}^T \varphi(\mathbf{x}_i) + b - y_i \leq \varepsilon + \xi_i^* \quad i = 1, 2, \dots, N \quad (6)$$

$$\xi_i \geq 0, \xi_i^* \geq 0 \quad (7)$$

This problem can be solved as a quadratic optimization problem with inequality constraints (Zhang et al., 2016). The high-dimensional weight factor  $\mathbf{W}$  is obtained as Eq.(8). Where,  $\beta_i^*$  and  $\beta_i$  are the Lagrangian multipliers by solving the quadratic problem. Then, the SVR function is written as Eq.(9). Where,  $K(\mathbf{x}_i - \mathbf{x})$  is the kernel function, transforming data  $\mathbf{x}$  into a higher dimensional feature space. In this study, RBF (Radial Basis Function) kernel function is selected for the data mapping (Li et al., 2009), as shown in Eq.(10).

$$\mathbf{W} = \sum_{i=1}^N (\beta_i^* - \beta_i) \varphi(\mathbf{x}_i) \quad (8)$$

$$f(\mathbf{x}) = \sum_{i=1}^N (\beta_i^* - \beta_i) K(\mathbf{x}_i - \mathbf{x}) + b \quad (9)$$

$$K(\mathbf{x}, \mathbf{y}) = e^{-\gamma \|\mathbf{x} - \mathbf{y}\|^2}, \gamma > 0 \quad (10)$$

- SVR model development

The output of the SVR model for the data-driven MPC during the fast DR event is the indoor air temperature ( $T_{in}^k$ ). The indoor air temperature is dominantly influenced by outdoor weather conditions and space usage in commercial buildings (Xu et al., 2019). The calendar information could well reflect the space usage schedule, e.g., occupants and equipment. Therefore, outdoor air temperature ( $T_{out}^k$ ) and time (hour) of a day ( $t$ ) are considered in the model, as shown in Eq.(11). Besides, chiller power demand at current  $k$  time step ( $P_{ch}^k$ ) and indoor air temperature of last time step ( $T_{in}^{k-1}$ ) are involved. The last time step of indoor temperature is to describe the dynamic of temperature changes during the DR event. The chiller power demand reflects the impacts of cooling supply on indoor temperature. Where,  $T_{in,rev}^k$  is the final indoor temperature predicted by MPC after the prediction result of SVR model ( $T_{in}^k$ ) is modified by a modification factor ( $\widehat{\theta}_k$ ) to address the unpredictable disturbances and model uncertainties. (in section 3.3).

$$T_{in}^k = f(P_{ch}^k, T_{out}^k, T_{in}^{k-1}, t) \quad (11)$$

$$T_{in,rev}^k = T_{in}^k + \widehat{e}_k \quad (12)$$

To improve the prediction performance of SVR for online control, two steps are added in this study before model training, i.e., data normalization and SVR hyperparameter optimization.

Data normalization: for improving the prediction efficiency and preventing individual data from overflowing, the dataset (inputs and outputs) are normalized by Eq.(12) before training. Where  $v_{max}$  and  $v_{min}$  are the corresponding maximum and minimum values.  $v'_i$  and  $v_i$  represent the normalized and original datasets of inputs and outputs, respectively. After the prediction results ( $G$ ) of SVR model obtained, the predicted values ( $G$ ) should be transformed into the actual prediction value  $\hat{q}$  by Eq.(13). Where  $q_{max}$  and  $q_{min}$  are the maximum and minimum values of prediction results.

$$v'_i = \frac{v_i - v_{min}}{v_{max} - v_{min}} \quad (12)$$

$$\hat{q} = q_{min} + G \cdot (q_{max} - q_{min}) \quad (13)$$

SVR hyperparameter optimization ( $\gamma$  and  $C$ ): In Eq.(4),  $C$  represents the tolerance of prediction error. A higher  $C$  will result in a lower prediction error but a higher risk of over-fitting and vice versa. In Eq.(10),  $\gamma$  is the parameter of kernel function to handle nonlinear regression by mapping the dataset into a high-dimensional feature space. To optimize these two parameters, the grid search method is used to exhaustively test the possible combination of  $\gamma$  and  $C$  by evaluating each case performance. Then the best combination is selected for the following SVR model development. To avoid the overfitting in the parameter optimization process,  $k$ -folds cross-validation is performed and  $k$  is set as 6 in this study.

- SVR model performance evaluation

To evaluate the performance, three performance indices are used, i.e., root means square error (RMSE), mean absolute error (MAE), and mean absolute percentage error (MAPE). The definitions of these three performance indices are shown in Eqs.(14-16). Where  $\widehat{Y}_t$  is the prediction value of the

SVR model.  $Y_i$  is the actual measurement.  $n$  is the total number of measurements.

$$RMSE = \sqrt{\frac{\sum_{i=1}^n (Y_i - \hat{Y}_i)^2}{n}} \quad (14)$$

$$MAE = \frac{\sum_{i=1}^n |Y_i - \hat{Y}_i|}{n} \quad (15)$$

$$MAPE = \frac{1}{n} \sum_{i=1}^n \frac{|Y_i - \hat{Y}_i|}{Y_i} \quad (16)$$

### 3.2.2 RC model

The RC model is regarded as a reference in this study to achieve a comparison with the SVM model for online control during fast DR events. The schematic of the building RC thermal model is shown in Fig.4, describing the heat exchanges and energy balances between outdoor, indoor and building envelop. This model is used to predict the indoor air temperature under a given chiller power demand. The RC model embedded into MPC is as the format of Eqs.(17-18).

$$X_{k+1} = A_d \cdot X_k + B_d \cdot u_k + E_d \cdot d_k \quad (17)$$

$$y_k = C_d \cdot X_k + \hat{e}_k \quad (18)$$

Where,  $A_d$ ,  $B_d$ ,  $C_d$ , and  $E_d$  are the coefficients. System state  $X_k = [T_{w,ex} \ T_{w,in} \ T_{im,1} \ T_{im,2} \ T_{in}]^T$ . The indoor air temperature can be obtained directly by measurement, while the other unmeasurable variables can be estimated by the Kalman filter (Afram & Janabi-Sharifi, 2014; Simon, 2006). Control input  $u_k = P_{ch}$  ( $P_{ch}$  is chiller power demand). The disturbance vector  $d_k = [I_{solar} \ T_{out} \ Q_{inter}]^T$ .  $y_k$  is the prediction output, i.e.,  $T_{in}$ . The detailed meanings of parameters in system state vector and disturbance vector can be found in Appendix A.

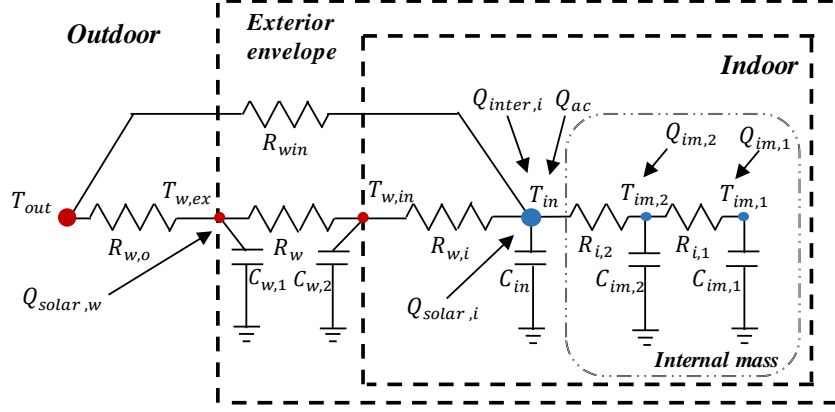


Fig.4 Heat fluxes and energy balances in building thermal model (Tang & Wang, 2019)

### 3.3 Model correction

In the above two models, the prediction result is further revised by a factor  $\widehat{e}_k$  to address the prediction errors and hence improve the accuracy. Its value is determined by the first-order exponential smoothing method, as shown by Eq.(19). The modification factor at  $(k+1)^{th}$  interval (i.e.,  $\widehat{e}_{k+1}$ ) is calculated by the prediction error ( $e_k$ ) and the value ( $\widehat{e}_k$ ) at  $k^{th}$  time step. Where  $\theta$  is a weighting factor ( $0 < \theta < 1$ ).  $e_k$  is prediction error obtained by comparing the actual measurement with the predicted value at  $k^{th}$  time step.  $\widehat{e}_k$  is the factor at  $k^{th}$  time step. At the start of the DR event, the initial value of  $\widehat{e}_k$  ( $k = 1$ ) is set as zero.

$$\widehat{e}_{k+1} = \theta * e_k + (1 - \theta) * \widehat{e}_k \quad (19)$$

### 3.4 Online control optimization

Three scenarios are considered for optimal control of chillers in fast DR events, i.e., minimum and smooth power demand, maximum and smooth power demand reduction, and maximum average power demand reduction. Different power demand controls would be required in different DR programs (Li et al., 2016). Meanwhile, a comprehensive comparison between the SVR-based MPC and RC-based MPC is achieved to test the performance of the proposed data-driven MPC. The optimization control of three scenarios are formulated as follows:

- Scenario 1: Minimum and smooth power demand control

Problem formulation: In scenario 1, chiller demand control during DR events provides a

minimum and smooth power demand profile while maintains indoor temperature acceptable. The objective function of this scenario is described as Eq.(20). The first item is to realize a smooth power demand control and the second is for minimizing the power demand. Where,  $\mathbf{P}_{ch}^k = [P_{ch}(k+1|k) \dots P_{ch}(k+N_p|k)]$ . The argument  $(k+N_p)|k$  means the prediction results at  $(k+N_p)^{th}$  considering the measurements up to  $k^{th}$  time step.  $\overline{P_{chiller}}$  is average predicted chiller demand over the prediction horizon ( $N_p$ ) at  $k^{th}$  step, as calculated by Eq.(21).  $\lambda_1$  is a weighting factor.  $N$  is the prediction horizon of the entire DR event and its value is based on the time step ( $step$ ) and time duration ( $D$ ) of the DR event, as shown in Eq.(23). Note that the prediction horizon ( $N_p$ ) at each sampling time is shrunk over the entire DR event, not a fixed value. Due to the characteristic of such fast DR events lasting for a short period, the shrunk prediction horizon can cover the rest of the DR event (i.e., from the next time step (i.e.,  $k+1$ ) to the end of DR event) to effectively grasp the dynamics of control states.

$$\min J_{RC,1} = \frac{1}{N_p} [(\mathbf{P}_{ch}^k - \overline{P_{chiller}}) \cdot (\mathbf{P}_{ch}^k - \overline{P_{chiller}})^T + \lambda_1 \cdot \mathbf{P}_{ch}^k \cdot \mathbf{P}_{ch}^{k,T}] \quad (20)$$

$$\overline{P_{chiller}} = \frac{1}{N_p} \sum_{t=k+1}^{k+N_p} P_{ch}(t|k) \quad (21)$$

$$N_p = N - k + 1 \quad (22)$$

$$N = D/step \quad (23)$$

The indoor temperature of DR event would be without violating maximum acceptable limit ( $T_{max}$ ), i.e., Eq.(24). Under the limited cooling supply in the DR event, there is no concern about indoor temperature lower limit ( $T_{min}$ ) (i.e., lower than original set-points) and hence  $T_{min}$  is set as the original set-point. The chiller power demand should be maintained within its capacity, i.e., between the minimum ( $P_{chiller,min}$ ) and maximum capacity ( $P_{chiller,max}$ ) of retained chillers (i.e., Eq.(25)). The optimized control variables of  $k^{th}$  time step is  $\mathbf{u}_k = [\mathbf{P}_{ch}^k] = [P_{ch}(k+1|k) \dots P_{ch}(k+N_p|k)]$ . But only the first value of  $P_{ch}(k+1|k)$  is sent out to be implemented at  $(k+1)^{th}$  time step.

$$T_{min} \leq T_{in}^k \leq T_{max} \quad (24)$$

$$P_{chiller,min} \leq \mathbf{u}_k \leq P_{chiller,max} \quad (25)$$

Online optimization: To solve the formulated problems, the quadratic program is used for the RC-based MPC to identify the optimal control solutions because the RC model is linear. In contrast, the SVR model is nonlinear, and therefore genetic algorithm (GA) is employed for online optimization due to its powerful ability for solving nonlinear optimization problems. GA is an evolutionary search algorithm via the process of natural selection. It makes a population of individuals evolve to an optimal solution by successive modifications. Three steps, i.e., selection, crossover, and mutation, are experienced to create the next generation based on the current generation at each modification (Tuhus-Dubrow & Krarti, 2010). To ensure the optimization performance of GA and search best possible optimal solutions, two efforts are made in this study:

(1) Shortened searching range of GA. Local convergency is a critical issue when using GA, which causes the solution converged to local optimum not global optimum, and therefore results in bad optimization performance. To alleviate this problem, the target control state (chiller power demand) is restricted within a narrow searching range. This is benefited by the characteristic of fast DR. At the start of such events, retained number of operating chillers (i.e.,  $m$ ) is optimized considering the constraints of indoor environment and then keeps unchanged in the entire events (the determination of retained chiller number can be found in (Tang et al., 2018)). So the searching range of chiller power demand is located in a narrow range of  $[(m-1)P - \beta, mP + \beta]$  rather than the range covering the cumulative capacity of all the operating chillers. Where  $P$  is the rated capacity of chillers;  $\beta$  is a safety factor, which is set as around half of rated chiller power to cover enough searching range.

(2) To address the constraint of indoor temperature when conducting the GA optimization, the penalty function is used to combine the constraint into the objective function, as shown in Eq.(26). Where,  $J_{RC,1}$  represents the objective function set for the RC-based MPC optimization in scenario 1.  $\epsilon_1$  is a weighting factor, making first and second terms in the objective function at a similar magnitude.  $J_{SVR,1}$  is the objective function for SVR-based MPC in scenario 1.

$$\min \quad J_{SVR,1} = J_{RC,1} + \epsilon_1 \cdot [\min(T_{in} - T_{max}, 0) - \min(T_{in} - T_{min}, 0)] \quad (26)$$

- Scenario 2: Maximum and smooth power demand reduction control

In scenario 2, chiller demand control during DR events provides a maximum and smooth power demand reduction compared with a given baseline. The objective function of this scenario is shown in Eqs.(27-29). In Eq.(27), the first part is to make power reduction stable and the second part is for a maximum power reduction. Where,  $\mathbf{P}_{ch,red}^k$  is the matrix of chiller power demand reduction from  $(k+1)^{th}$  time step to the end of DR event, i.e.,  $\mathbf{P}_{ch,red}^k = [P_{ch,red}(k+1|k) \cdots P_{ch,red}(k+N_p|k)]$ .  $P_{ch}^k$  is the optimized chiller power demand at  $k^{th}$  time step.  $P_{ch,base}^k$  is the baseline of chiller power demand without any DR control (i.e., original power demand). The constraints are indoor temperature limits and chiller capacity, which are the same as scenario 1, as defined in Eqs.(24-25). Using penalty function for handling the indoor temperature constraints, Eq.(30) is the objective function of SVR-based MPC using genetic algorithm. Where,  $J_{RC,2}$  represents the objective function set for the RC-based MPC optimization in scenario 2.  $\mathcal{E}_2$  is a weighting factor.  $J_{SVR,2}$  is the objective function for SVR-based MPC in scenario 2.

$$\min J_{RC,2} = \frac{1}{N_p} [(\mathbf{P}_{ch,red}^k - \overline{P_{ch,red}}) \cdot (\mathbf{P}_{ch,red}^k - \overline{P_{ch,red}})^T - \lambda_2 \cdot \mathbf{P}_{ch,red}^k \cdot \mathbf{P}_{ch,red}^{k,T}] \quad (27)$$

$$P_{ch,red}^k = P_{ch,base}^k - P_{ch}^k \quad (28)$$

$$\overline{P_{ch,red}} = \frac{1}{N_p} \sum_{t=k+1}^{k+N_p} P_{ch,red}(t|k) \quad (29)$$

$$\min J_{SVR,2} = J_{RC,2} + \mathcal{E}_2 \cdot [\min(T_{in} - T_{max}, 0) - \min(T_{in} - T_{min}, 0)] \quad (30)$$

- Scenario 3: Maximum average power demand reduction control

In scenario 3, chiller demand control during the DR events is for a maximum average power reduction compared with baseline and simultaneously keeps indoor temperature accepted. At  $k^{th}$  sampling time, the objective function is shown in Eq.(31). Where,  $\mathbf{P}_{ch}^k$  and  $\mathbf{P}_{ch,base}^k$  are optimized chiller demand and corresponding baseline from  $(k+1)^{th}$  time step to the end of DR event. The constraints are indoor temperature limits and chiller capacity, as defined in Eqs. (24-25). Eq.(32) is the objective function of SVR-based MPC using genetic algorithm that indoor temperature constraints are involved in using the penalty function. Where,  $J_{RC,3}$  represents the objective function set for the RC-

based MPC optimization in scenario 3.  $\epsilon_3$  is a weighting factor, of which value is set based on the rated chiller power demand.  $J_{SVR,3}$  is the objective function for SVR-based MPC in scenario 3.

$$\min J_{RC,3} = \frac{1}{N_p} (\mathbf{P}_{chiller}^k - \mathbf{P}_{ch,base}^k) \quad (31)$$

$$\min J_{SVR,3} = J_{RC,3} + \epsilon_3 \cdot [\min(T_{in} - T_{max}, 0) - \min(T_{in} - T_{min}, 0)] \quad (32)$$

#### 4. Test platform

Computer-based dynamic simulation is an effective way to test and validate online optimal control strategies before implementation. A co-simulation test platform on TRNSYS-MATLAB (Klein et al., 2006) is set up to validate the SVR-based MPC in fast DR events. The detailed dynamic models of components in a central air-conditioning system are involved in the platform (Wang, 1998). The centrifugal chiller model is employed for the chiller dynamic and performance, which is mainly based on impeller tip speed, impeller exhaust area, impeller blade angle, and thirteen co-efficient parameters. The compression process in the compressor, the heat transfer process in the evaporator and the condenser are simulated in the model. Air handling unit (AHU) model in ref. (Wang, 1998) is used, which is based on classical number of transfer unit (NTU) and heat transfer effectiveness ( $\epsilon$ ) methods to realize the heat transfer calculation. Both dry and wet regions are considered for the calculation of heat conversion coefficient on the air side. The energy performance and characteristics of pump at various speeds are simulated using fourth-order poly-nominal function as described in ref. (Wang, 1998).

System configuration: the central chiller plant for the tests is a typical primary constant-secondary variable chilled water system. It is modified on basis of a central air-conditioning system of a high-rise commercial building in Hong Kong. The system is shown in Fig.1. Six identical chillers with a rated cooling capacity of 4080 kW are employed in the chiller plant. Every chiller is equipped with a constant-speed primary pump with a capacity of 172.5 L/s. The chilled water pumps in the secondary loop of the system are variable speed pumps.

Model development: to train the SVR model, system identification is performed on the TRNSYS

test platform. The indoor temperature setpoints, which are generated by a random sequence, are regarded as the excitation input to obtain the system dynamics. The upper and lower bounds of random sequence are 23.5°C and 27.5°C respectively, which are 0.5°C higher/lower than the acceptable range in this study, [24°C, 27°C]. The hyperparameter combination of  $\gamma$  and  $C$  in the SVR model are 2 and 16 optimized by grid search in  $k$ -folds cross-validation as illustrated in section 3.2.1 ( $k$  is set as 6). The values of  $R$  and  $C$  in RC model are presented in Table 1, and the model accuracy has been validated in ref.(Tang & Wang, 2019). The values of coefficient matrixes  $A_d$ ,  $B_d$ ,  $E_d$ , and  $C_d$  in the discrete-time state-space model for RC-based MPC are given in Appendix B.

Table 1 Parameters of  $R$  and  $C$  for the tests

	$R_{w,o}$ ( $m^2K/W$ )	$R_w$ ( $m^2K/W$ )	$R_{w,in}$ ( $m^2K/W$ )	$R_{i,1}$ ( $m^2K/W$ )	$R_{i,2}$ ( $m^2K/W$ )
Value	0.0942	0.0892	0.0039	0.0024	0.0107
	$R_{win}$ ( $m^2K/W$ )	$C_{w,1}$ ( $J/(m^2K)$ )	$C_{w,2}$ ( $J/(m^2K)$ )	$C_{im,1}$ ( $J/(m^2K)$ )	$C_{im,2}$ ( $J/(m^2K)$ )
Value	0.0105	$9.229*10^8$	$9.997*10^8$	$8.811*10^7$	$9.725*10^7$

Test settings: the DR period for the urgent request of power grids is assumed to be 2 hours from 2:00 pm to 4:00 pm. Once the DR signal is received from power grids, DR control will shut down one of four operating chillers and remain three chillers operating accordingly. The outdoor weather condition of the test day is shown in Fig.5, which is a typical summer day in Hong Kong. The set-point of indoor air temperature is 24°C under normal system operation, while under DR control, the maximum indoor temperature accepted is 27°C (3°C increase). The parameters of Population Size, Max-Generation, and Function-Tolerance in GA for the online optimization of SVR-based MPC are set as values of 100, 160, and  $10^{-6}$  respectively. The RC-based MPC for the online optimal control problem is solved using the YALMIP optimization toolbox (Lofberg, 2004) with Gurobi solver (Optimization, 2014). The time step of the dynamic simulation is set as 1 second. The sampling time for the online two MPC strategies is 15min, i.e., the set-points are updated every 15min.

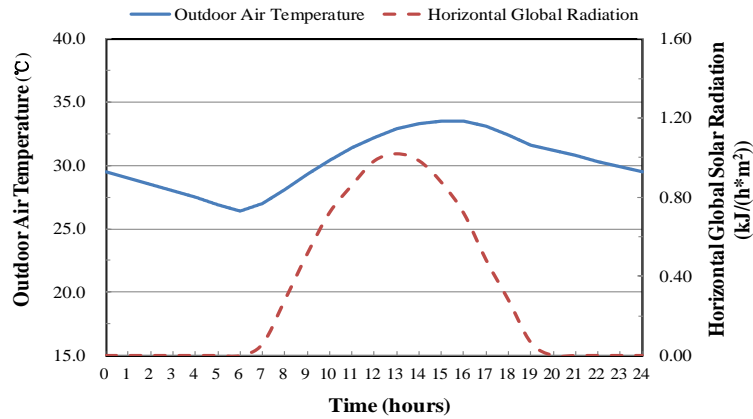


Fig.5 Outdoor weather condition on the test day

## 5. Results and discussion

### 5.1 Model validation and necessity of MPC

#### Model validation

The data of five summer workdays in a week were selected to validate the prediction of the SVR model. The predicted values by RC and SVR as well as actual indoor temperatures are shown in Fig.6. The results of three evaluation indices (MAE, MAPE, and RMSE) are presented in Table 2 to describe the model accuracy. The SVR model could well predict the system dynamic of indoor temperature and even is a little better than the RC model.

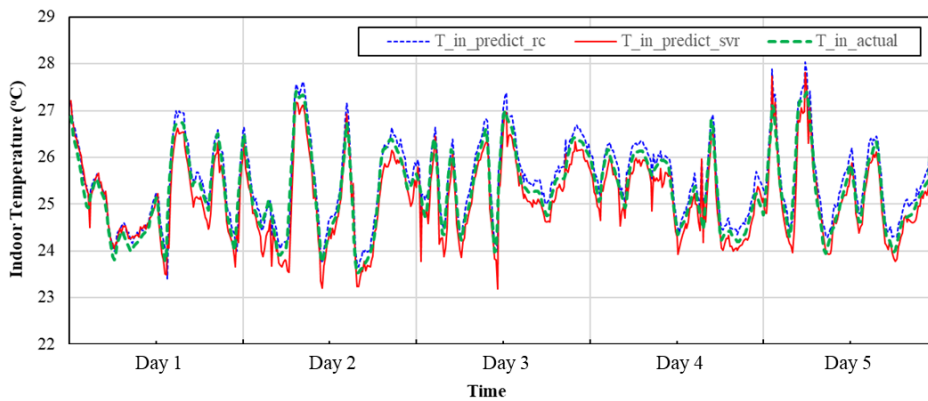


Fig.6 Predicted indoor temperature profiles using RC model and SVR model compared with actual measurements

Table 2 Evaluation indices of SVR model and RC model

	MAE (°C)	MAPE (%)	RMSE (°C)
SVR model	0.108	0.429	0.328
RC model	0.251	0.892	0.460

### Necessity of MPC for fast DR optimal control

Without predictive controls, the indoor temperature and chiller power demand cannot be controlled as expected simultaneously (Tang & Wang, 2019). If maintaining the indoor temperature at the upper limit, the chiller will be operating passively to meet the cooling demand rather than at the expected load profile for DR programs. Similarly, if chiller power demand is operating without considering system dynamics to predict the indoor temperature response, the indoor temperature will deviate from the optimal condition obviously, which would cause maximum indoor temperature increase to unacceptable at a higher risk. In addition, MPC can relieve the serious fluctuation resulted from suddenly significant changes of switching off operating chillers directly at the start of such fast DR events.

### ***5.2 Analysis of control performance during the DR event --- Scenario 1***

In scenario 1, the control performance was evaluated considering two aspects: smooth and minimum chiller power demand and indoor air temperature below the acceptable upper limit (i.e., 27°C). Fig.7(a) presents the optimized power demand set-points of chiller in the DR event by two MPC approaches. The difference in the results of two methods was within a small range. The standard deviation of chiller power demand during the event that could quantify the smoothness of chiller power demand was 89.1kW using SVR-based MPC, near to the result of 67.9kW using RC-based MPC. Although the difference between the maximum and minimum power demands was 1244kW, this was induced by the sudden change of system operation at the start of the DR event (switching off operating chillers directly). After the system reached the new balance, the chiller power demand fluctuation was relieved significantly and well followed the optimized set-points using SVR-based MPC, as shown in Fig.7(b).

Fig.8 shows the indoor temperatures of the DR event using two MPC approaches. During the DR event, the maximum indoor temperature was almost below the upper limit using the SVR-based MPC. (only a short period exceeded the limit with a maximum value of 27.2°C, which also demonstrated no potential for a further power reduction). In Table 3, the average power demand reduction of 570kW (i.e., 19.3%) was achieved by SVR-based MPC, which was similar to the RC-based MPC.

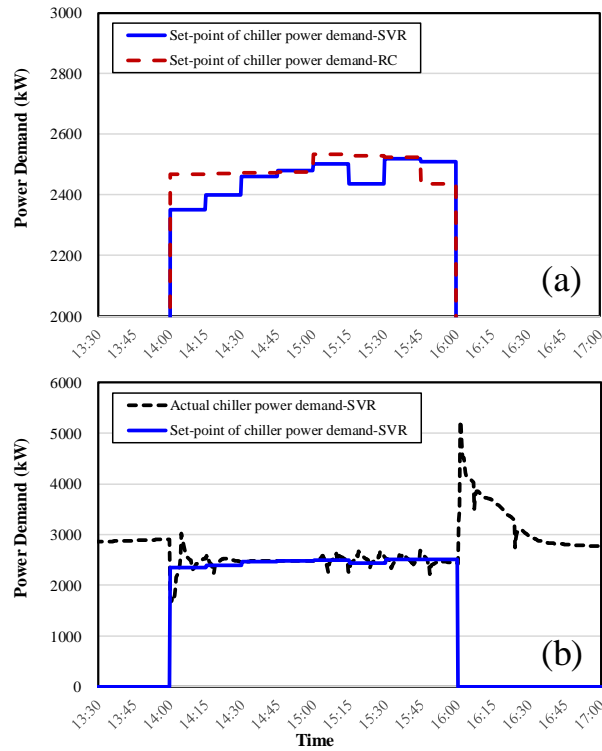


Fig.7 Set-points of chiller power demand optimized by SVR-based MPC and RC-based MPC (a), and actual chiller power demand using SVR-based MPC (b) in the DR event– Scenario 1

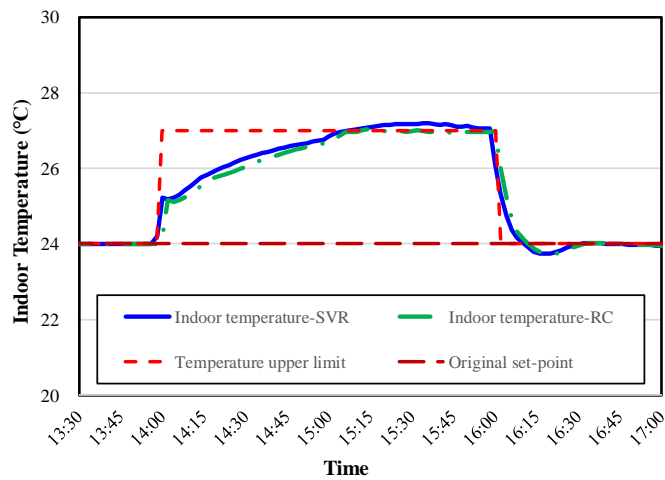


Fig.8 Indoor temperature profiles during the DR event using SVR-based and RC-based MPC approaches – Scenario 1

Table 3 Control performance of using SVR-based and RC-based MPC approaches – Scenario 1

	Actual chiller power demand						Indoor temperature
	Maximum (kW)	Minimum (kW)	Standard deviation (kW)	Average demand (kW)	Average reduction (kW)	Percentage (%)	Maximum (°C)
SVR-based MPC	3019	1775	89.1	2377	570	19.3	27.2
RC-based MPC	3137	2017	67.9	2449	498	16.9	27.0

\* Baseline of chiller power demand in this scenario is simplified as the value just before the DR event (i.e., 2947kW)

### 5.3 Analysis of control performance during the DR event --- Scenario 2

In scenario 2, the objective of DR control was to achieve a maximum and smooth (stable) power reduction contributed by chillers with ensuring the indoor temperature below the upper limit. The power reduction was obtained based on a pre-defined baseline profile of building operating without any DR controls. In this study, the baseline was not the focus and hence assumed to be known during the DR event.

Fig.9(a) presents the set-points of chiller power demand optimized by two MPC approaches during the fast DR event. The optimized results were similar with a few differences between these two approaches. The standard deviation of power demand reduction during the event was 76.6kW using SVR-based MPC, even better than that of 81.2kW using the RC-based approach. The difference between the maximum and minimum power demand reduction was obvious, caused by the sudden change of system operation at the start of the DR event. About 10min later, actual chiller power demand reduction could be stable and well follow the optimized set-points of SVR-based MPC, as shown in Fig.9(b).

Fig.10 shows the indoor temperatures of the DR event using two MPC approaches. During the DR event, the maximum indoor temperature was almost below the upper limit using SVR-based MPC

(with a maximum value of 26.8°C). In Table 4, the average power demand reduction of 528kW (i.e., 17.2%) was achieved by SVR-based MPC, which was similar to the RC-based MPC, but the maximum temperature was lower than that of RC-based MPC. Considering the indoor temperature at the last half hour of the DR event was around the limit value, the power reduction was achieved almost at the maximum.

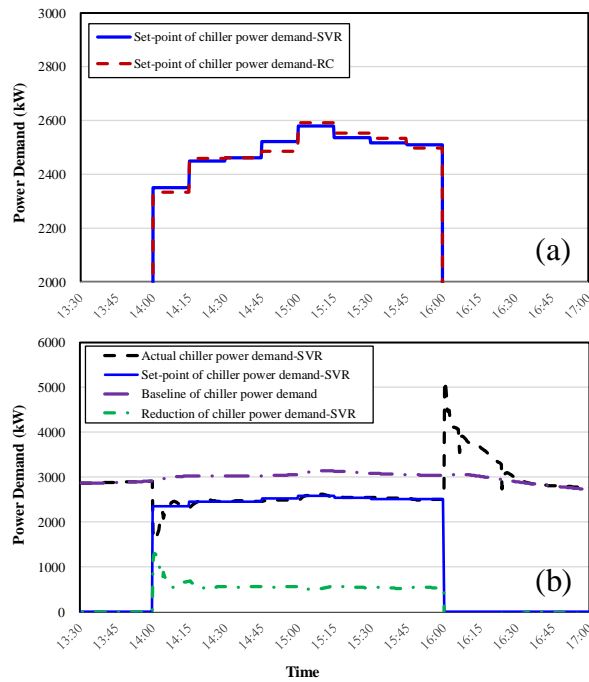


Fig.9 Set-points of chiller power demand optimized by SVR-based MPC and RC-based MPC (a), and actual chiller power demand using SVR-based MPC approach (b) in the DR event –Scenario 2

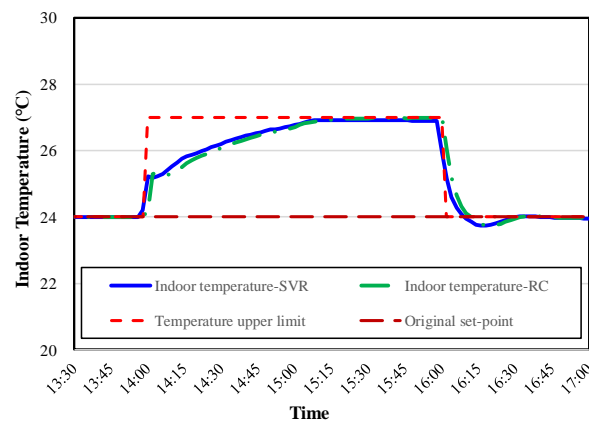


Fig.10 Indoor temperature profiles during the DR event using SVR-based and RC-based MPC approaches – Scenario 2

Table 4 Control performance of using SVR-based and RC-based MPC approaches – Scenario 2

	Actual power demand						Indoor temperature
	Maximum reduction (kW)	Minimum reduction (kW)	Standard deviation (kW)	Average demand (kW)	Average reduction (kW)	Percentage (%)	Maximum (°C)
SVR-based MPC	1187	501	76.6	2542	528	17.2	26.8
RC-based MPC	1209	487	81.2	2498	572	18.6	26.9

\* Baseline of average chiller power demand in this scenario is 3070kW

#### 5.4 Analysis of control performance during the DR event --- Scenario 3

In scenario 3, the DR control was to maximize the average chiller power reduction by maintaining the indoor temperature below the upper limit (27°C). The main difference in this scenario between the above two cases was that the power demand control was simplified as a value to evaluate the control performance rather than an expected profile. This case was therefore easier and more practical for the real applications. The baseline of average chiller power demand was assumed to be known in this scenario.

Fig. 11(a) presents the optimized set-points of chiller power demand using two approaches during the DR event. The difference between the optimized results using these two methods was kept within a very small range. The actual chiller power demand could well track the optimized chiller power demand set-points optimized by SVR-based MPC, as shown in Fig. 11(b). The average power demand during the DR event was 2394 kW, about 22.0% of power reduction achieved by SVR-based MPC which was similar to that of RC-based MPC (i.e., 22.3%).

Evaluation of whether average power reduction reached its maximum could be based on the indoor temperature profile. The best condition with maximum reduction was to maintain the indoor temperature operating at the upper limit (27°C) in the entire DR period. This meant that there was no potential for a further power reduction at any time of the DR event. The time duration of indoor temperature over 26.5°C was calculated to reflect the degree of achieved maximum power reduction.

As shown in Fig.12, the temperature was almost maintained at its upper limit using SVR-based MPC with a duration of 112 minutes over 26.5°C in the two hours DR event, which was better than using RC-based MPC (i.e., 102min). As a result, more reduction was achieved by SVR-based MPC but with a similar maximum indoor temperature (27.07°C) compared with the results using RC-based MPC.

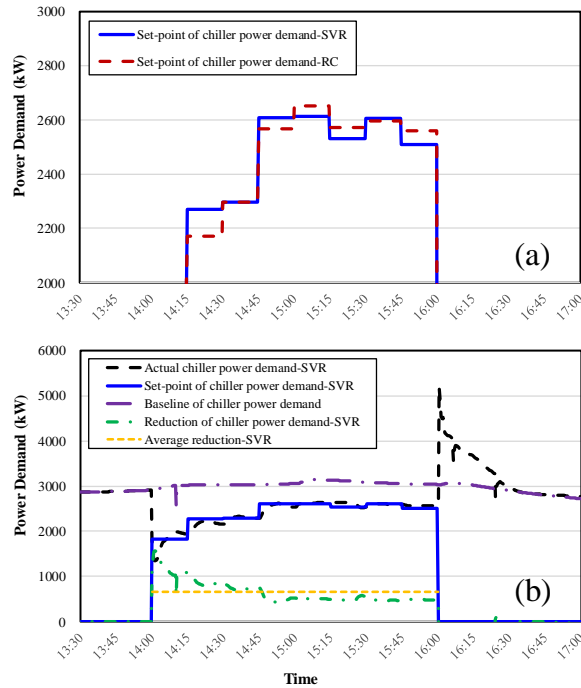


Fig.11 Set-points of chiller power demand optimized by SVR-based MPC and RC-based MPC (a), and actual chiller power demand using SVR-based MPC strategy (b) in the DR event – Scenario 3

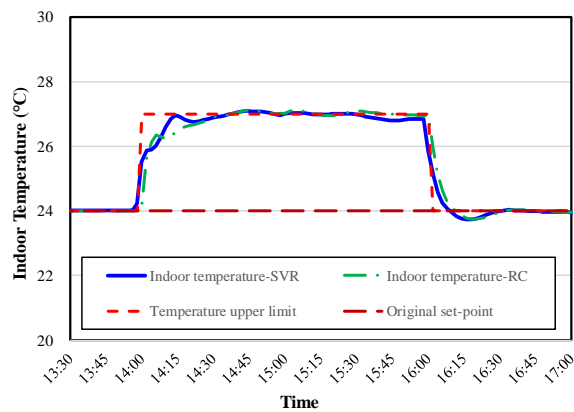


Fig.12 Indoor temperature profiles during the DR event using SVR-based and RC-based MPC approaches – Scenario 3

Table 5 Control performance of using SVR-based and RC-based MPC approaches – Scenario 3

	Actual power demand			Indoor temperature	
	Average demand (kW)	Average reduction (kW)	Percentage (%)	Maximum (°C)	Time Duration (min)
SVR-based MPC	2394	676	22.0	27.07	112
RC-based MPC	2385	685	22.3	27.12	102

\* Baseline of average chiller power demand in this scenario is 3070kW.

### 5.5 Comparison of two methods

According to the results, SVR can get a relatively better prediction performance of building dynamics than RC model because RC model needs some inputs that are not easily accurately measured such as internal heat gain while SVR is capable of capturing the nonlinear relations only driven from inputs and output data. According to the three scenarios, SVR-based MPC can achieve a similar control performance as RC-based MPC method. Although more accurate prediction is obtained by SVR, the optimization process using GA will get an approximate solution rather than an exact solution, which would negatively influence the control performance. Besides, the SVR-based MPC can effectively handle the suddenly significant change at the start of DR events, which more uncertain and serious disturbance on the control system compared with other normal conditions of parameter changes (e.g., weather data, occupant number), and therefore the robustness of the proposed method is demonstrated.

The advantages of SVR-based MPC when applied for fast DR controls, compared with RC-based MPC, include: (1) the flexible structure of models. The SVR-based MPC control could be easily adjusted and applied for other targeted buildings, but the RC-based model is specialized for a specific control system and difficult to be extended even in the same building; (2) the saving in efforts and time costs for modeling. SVR-based MPC can reduce the efforts caused by considering detailed system dynamics in the developing process of RC-based models; (3) less information and data for SVR model inputs without sacrificing the prediction accuracy. Only four inputs are required, i.e., chiller power demand, outdoor and indoor temperatures, and time (hour of a day), which are easily measurable. Contrarily, RC model needs internal heat gain, solar radiation, and parameters such as split

radiative/convective heat gain of solar radiation additionally, which are difficult to be measured and obtained accurately.

## 6. Conclusion

Demand response (DR) is an effective method to benefit and strengthen the health operation of power grids. In commercial buildings, shutting down part of operating chillers could fulfill the need of immediate power reduction for smart grids. In such special events, the advanced control strategy would be adopted for the optimal control of an acceptable indoor environment and expected power demand. This study, therefore, bridged the gap of using SVR-based data-driven model predictive control (MPC) for fast DR events. To enhance the control performance, the data-driven MPC was equipped with optimized hyperparameters, penalty function for constraints of indoor temperature, and shortened searching range for genetic algorithm optimization fully considering the characteristics of such DR events. The control performance was compared with RC-based MPC under three different scenarios.

Test results show that the SVR outperforms the RC model on the prediction of building dynamics due to its nonlinear regression ability and no inputs required of difficulty to be measured. SVR-based MPC approach could optimize the controls for chiller power demand and indoor temperature simultaneously under three different control scenarios. The results in detail are presented as follows. Overall, the proposed SVR-based MPC can achieve a similar better control performance as using RC-based method for the optimal controls of fast DR events. From the perspectives of modeling effort and extendable ability, SVR-based MPC method is advantageous over RC-based MPC for the control of fast DR events.

- In scenario 1 of minimum and smooth power demand control, using SVR-based MPC, 19.3% of power reduction was achieved with a standard deviation of chiller power demand of 89.1kW, which was approaching the results of RC-based MPC.
- In scenario 2 of maximum and smooth power demand reduction control, using SVR-based MPC, 17.2% of power reduction was achieved with a standard deviation of chiller power demand

reduction of 76.6kW and a maximum indoor temperature of about 26.8°C, which were a little better controlled than RC-based MPC.

- In scenario 3 of maximum average power demand reduction control, the SVR-based MPC kept the indoor temperature almost at its upper limit to maximize the average power demand reduction (22.0%) in the DR event, which compared with using RC-based MPC, a similar power reduction was achieved but with a lower maximum indoor temperature.

## Appendix

### A. Development of the RC model for MPC

According to Fig.4, the heat exchanges and energy balances between outdoor, indoor and building envelop are presented in Eqs.(a-1~a-5) (Tang & Wang, 2019).

$$C_{w,1} \frac{dT_{w,ex}}{dt} = \frac{T_{out}-T_{w,ex}}{R_{w,o}} - \frac{T_{w,ex}-T_{w,in}}{R_w} + Q_{solar,w} \quad (a-1)$$

$$C_{w,2} \frac{dT_{w,in}}{dt} = \frac{T_{w,ex}-T_{w,in}}{R_w} - \frac{T_{w,in}-T_{in}}{R_{w,i}} \quad (a-2)$$

$$C_{im,1} \frac{dT_{im,1}}{dt} = \frac{T_{im,2}-T_{im,1}}{R_{i,1}} + Q_{im,1} \quad (a-3)$$

$$C_{im,2} \frac{dT_{im,2}}{dt} = \frac{T_{im,1}-T_{im,2}}{R_{i,1}} - \frac{T_{im,2}-T_{in}}{R_{i,2}} + Q_{im,2} \quad (a-4)$$

$$C_{in} \frac{dT_{in}}{dt} = \frac{T_{im,2}-T_{in}}{R_{i,2}} + \frac{T_{w,in}-T_{in}}{R_{w,i}} + \frac{T_{out}-T_{in}}{R_{win}} + Q_{inter,i} - Q_{ac} + Q_{solar,i} \quad (a-5)$$

where, the values of  $R$  and  $C$  are determined by training historical data by genetic algorithm.  $T$  is temperature. Indoor air, outdoor air, exterior wall, internal wall surface, external wall surface, window, and internal mass are represented by the subscripts of  $i$ ,  $out$ ,  $w$ ,  $in$ ,  $ex$ ,  $win$  and  $im$ , respectively.  $Q_{solar}$  is solar heat gain.  $Q_{inter,i}$  is internal heat gain.  $Q_{im}$  is the radiation heat.  $Q_{ac}$  is the cooling demand provided by the central air-conditioning systems (i.e.,  $Q_{dem}$ ), which is determined by chiller power demand ( $P_{ch}$ ) and corresponding  $COP$  (coefficient of performance), as shown in Eq.(a-11).

$$Q_{solar,w} = \alpha I_{solar} \quad (a-6)$$

$$Q_{solar,i} = \beta_i \cdot SHGC \cdot I_{solar} \quad (a-7)$$

$$Q_{im,1} = Q_{im,2} = b \cdot (Q_{solar,im} + Q_{inter,im}) \quad (a-8)$$

$$Q_{solar,im} = \beta_{im} \cdot SHGC \cdot I_{solar} \quad (a-9)$$

$$Q_{inter,im} = \mu \cdot Q_{inter} \quad (a-10)$$

$$Q_{dem} = P_{ch} \cdot COP \quad (a-11)$$

where,  $I_{solar}$  is global solar radiation, obtained from weather data.  $\beta$ ,  $b$ , and  $\mu$  represent the pre-set ratio of split radiative/convective heat gain.  $\alpha$  denotes the absorptance of the surface of solar radiation.  $SHGC$  is solar heat gain coefficient.

The RC model is reformatted as a linear continuous-time state-space model in Eq.(a-12). Where system state vector  $x = [T_{w,ex} \ T_{w,in} \ T_{im,1} \ T_{im,2} \ T_{in}]^T$ . Control input vector  $u = [P_{ch}]^T$ . Disturbance vector  $d = [I_{solar} \ T_{out} \ Q_{inter}]^T$ . For online control, the continuous-time state-space model needs to be converted into the discrete-time state-space model (i.e., Eqs.(17-18)) based on the sampling time.

$$dx/dt = a \cdot x + b \cdot u + e \cdot d \quad (a-12)$$

System matrix  $a$ :

$$a = \begin{pmatrix} \frac{-1}{C_{w,1}R_{w,o}} + \frac{-1}{C_{w,1}R_w} & \frac{1}{C_{w,1}R_w} & 0 & 0 & 0 \\ \frac{1}{C_{w,2}R_w} & \frac{-1}{C_{w,2}R_w} + \frac{-1}{C_{w,2}R_{w,i}} & 0 & 0 & \frac{1}{C_{w,2}R_{w,i}} \\ 0 & 0 & \frac{-1}{C_{im,1}R_{i,1}} & \frac{1}{C_{im,1}R_{i,1}} & 0 \\ 0 & 0 & \frac{1}{C_{im,2}R_{i,1}} & \frac{-1}{C_{im,2}R_{i,1}} + \frac{-1}{C_{im,2}R_{i,2}} & \frac{1}{C_{im,2}R_{i,2}} \\ 0 & \frac{1}{C_{in}R_{w,i}} & 0 & \frac{1}{C_{in}R_{i,2}} & \frac{-1}{C_{in}R_{i,2}} + \frac{-1}{C_{in}R_{w,i}} + \frac{-1}{C_{in}R_{win}} \end{pmatrix}_{5 \times 5};$$

$$\text{Input matrix } b: b = \begin{pmatrix} 0 \\ 0 \\ 0 \\ 0 \\ \frac{-COP}{C_{in}} \end{pmatrix}_{5 \times 1};$$

$$\text{Disturbance matrix } e: e = \begin{pmatrix} \frac{a}{c_{w,1}} & \frac{1}{c_{w,1}R_{w,o}} & 0 \\ 0 & 0 & 0 \\ \frac{b\beta_{im}SHGC}{c_{im,1}} & 0 & \frac{b\mu}{c_{im,1}} \\ \frac{b\beta_{im}SHGC}{c_{im,2}} & 0 & \frac{b\mu}{c_{im,2}} \\ \frac{\beta_i SHGC}{c_{in}} & \frac{1}{c_{in}R_{win}} & \frac{1-\mu}{c_{in}} \end{pmatrix}_{5 \times 3}.$$

### B. Parameters of the discrete-time state-space model for MPC

$$\text{Matrix } A_d = \begin{pmatrix} 9.998 \times 10^{-1} & 1.093 \times 10^{-5} & 0 & 0 & 0 \\ 1.009 \times 10^{-5} & 9.989 \times 10^{-1} & 0 & 0 & 6.948 \times 10^{-7} \\ 0 & 0 & 9.958 \times 10^{-1} & 4.191 \times 10^{-3} & 0 \\ 0 & 0 & 3.796 \times 10^{-3} & 9.955 \times 10^{-1} & 2.571 \times 10^{-6} \\ 0 & 5.789 \times 10^{-1} & 0 & 2.084 \times 10^{-1} & 9.403 \times 10^{-7} \end{pmatrix}_{5 \times 5}$$

$$\text{Matrix } B_d: B_d = \begin{pmatrix} 0 \\ 0 \\ 0 \\ 0 \\ -1.003 \times 10^{-2} \end{pmatrix}_{5 \times 1}$$

$$\text{Matrix } E_d: E_d = \begin{pmatrix} 7.800 \times 10^{-7} & 1.034 \times 10^{-5} & 0 \\ 0 & 0 & 0 \\ 1.788 \times 10^{-6} & 0 & 2.555 \times 10^{-6} \\ 2.293 \times 10^{-6} & 0 & 3.276 \times 10^{-6} \\ 7.808 \times 10^{-4} & 2.119 \times 10^{-1} & 1.115 \times 10^{-3} \end{pmatrix}_{5 \times 3}$$

$$\text{Matrix } C_d: C_d = (0 \ 0 \ 0 \ 0 \ 1)_{1 \times 5}$$

## 7. Acknowledgments

The authors gratefully acknowledge the support of this research by the National Natural Science Foundation of China (No. 51908365) and the Philosophical and Social Science Program of Guangdong Province (GD18YGL07).

## References

- Afram, A., & Janabi-Sharifi, F. (2014). Theory and applications of HVAC control systems—A review of model predictive control (MPC). *Building and Environment*, 72, 343-355.
- Ahmad, M. W., Reynolds, J., & Rezgui, Y. (2018). Predictive modelling for solar thermal energy systems: A comparison of support vector regression, random forest, extra trees and regression trees. *Journal of Cleaner Production*, 203, 810-821.
- Arnold, G. W. (2011). Challenges and opportunities in smart grid: A position article. *Proceedings of*

*the IEEE*, 99(6), 922-927.

Avci, M., Erkoç, M., Rahmani, A., & Asfour, S. (2013). Model predictive HVAC load control in buildings using real-time electricity pricing. *Energy and Buildings*, 60, 199-209.

Chen, Y., Xu, P., Chu, Y., Li, W., Wu, Y., Ni, L., Bao, Y., & Wang, K. (2017). Short-term electrical load forecasting using the Support Vector Regression (SVR) model to calculate the demand response baseline for office buildings. *Applied Energy*, 195, 659-670.

Cui, B., Wang, S., Yan, C., & Xue, X. (2015). Evaluation of a fast power demand response strategy using active and passive building cold storages for smart grid applications. *Energy Conversion and Management*, 102, 227-238.

Depuru, S. S. S. R., Wang, L., Devabhaktuni, V., & Gudi, N. (2011). Smart meters for power grid - Challenges, issues, advantages and status. 2011 IEEE/PES Power Systems Conference and Exposition. Electrical and Mechanical Services Department (EMSD) of Hong Kong Government. Hong Kong Energy End-use Data, 2014. Available at: <https://data.gov.hk/en-data/dataset/hk-emsd-emsd1-energy-end-use-data-2014>.

Fan, C., Xiao, F., & Yan, D. (2021). Advanced data analytics for building energy modeling and management. *Building Simulation*, 14(1), 1-2.

Huang, G., Wang, S., & Xu, X. (2009). A robust model predictive control strategy for improving the control performance of air-conditioning systems. *Energy Conversion and Management*, 50(10), 2650-2658.

Killian, M., & Kozek, M. (2016). Ten questions concerning model predictive control for energy efficient buildings. *Building and Environment*, 105, 403-412.

Klein, S.A., Beckman, W.A., Mitchell, J.W., Duffie, J.A., Duffie, N.A., Freeman, T.L., Mitchell, J.C., Braun, J.E., Evans, B.L., Kummer, J.P., Urban, R.E., Fikesel, A., Thornton, J.W., Blair, N.J., Williams, P.M., Bradley, D.E., McDowell, T.P., Kummert, M., Arias, D.A.. TRNSYS, a transient simulation program, 2006. (University of Wisconsin-Madison, USA: Solar Energy Laboratory, version 16). Available at: <http://web.mit.edu/parmstr/Public/Documentation/08-ProgrammersGuide.pdf>. (last viewed date: July 2, 2018)

Kolokotsa, D., Rovas, D., Kosmatopoulos, E., & Kalaitzakis, K. (2011). A roadmap towards intelligent net zero-and positive-energy buildings. *Solar Energy*, 85(12), 3067-3084.

Li, Q., Meng, Q., Cai, J., Yoshino, H., & Mochida, A. (2009). Predicting hourly cooling load in the building: A comparison of support vector machine and different artificial neural networks. *Energy Conversion and Management*, 50(1), 90-96.

Li, S., Peng, J., Tan, Y., Ma, T., Li, X., & Hao, B. (2020). Study of the application potential of photovoltaic direct-driven air conditioners in different climate zones. *Energy and Buildings*, 226, 110387.

Li, W., Xu, P., & Jiao, F. (2016). Optimal demand response strategy of a portfolio of multiple commercial buildings: Methods and a case study. *Science and Technology for the Built Environment*, 22(6), 655-665.

- Lofberg, J (2004). A toolbox for modeling and optimization in MATLAB. 2004 IEEE International Conference on Robotics and Automation.
- Mai, W., & Chung, C. (2014). Economic MPC of aggregating commercial buildings for providing flexible power reserve. *IEEE Transactions on Power Systems*, 30(5), 2685-2694.
- Morari, M., & Lee, J. H. (1999). Model predictive control: past, present and future. *Computers & Chemical Engineering*, 23(4-5), 667-682.
- Motegi, N., Piette, M. A., Watson, D. S., Kiliccote, S., & Xu, P. (2007). Introduction to commercial building control strategies and techniques for demand response. *Lawrence Berkeley National Laboratory LBNL-59975*.
- Oldewurtel, F., Parisio, A., Jones, C. N., Gyalistras, D., Gwerder, M., Stauch, V., Lehmann, B., & Morari, M. (2012). Use of model predictive control and weather forecasts for energy efficient building climate control. *Energy and Buildings*, 45, 15-27.
- Olivieri, S. J., Henze, G. P., Corbin, C. D., & Brandemuehl, M. J. (2013). Evaluation of commercial building demand response potential using optimal short-term curtailment of heating, ventilation, and air-conditioning loads. *Journal of Building Performance Simulation*, 7(2), 100-118.
- Optimization, G. (2014). Inc., "Gurobi optimizer reference manual," 2015. URL: <http://www.gurobi.com>.
- Paniagua-Tineo, A., Salcedo-Sanz, S., Casanova-Mateo, C., Ortiz-García, E., Cony, M., & Hernández-Martín, E. (2011). Prediction of daily maximum temperature using a support vector regression algorithm. *Renewable Energy*, 36(11), 3054-3060.
- Pérez-Lombard, L., Ortiz, J., & Pout, C. (2008). A review on buildings energy consumption information. *Energy and Buildings*, 40(3), 394-398.
- Pourjafari, E., & Reformat, M. (2019). A support vector regression based model predictive control for volt-var optimization of distribution systems. *IEEE Access*, 7, 93352-93363.
- Ran, F., Gao, D.-c., Zhang, X., & Chen, S. (2020). A virtual sensor based self-adjusting control for HVAC fast demand response in commercial buildings towards smart grid applications. *Applied Energy*, 269, 115103.
- Simon, D. (2006). *Optimal state estimation: Kalman, H infinity, and nonlinear approaches*. John Wiley & Sons.
- Smarra, F., Jain, A., de Rubeis, T., Ambrosini, D., D'Innocenzo, A., & Mangharam, R. (2018). Data-driven model predictive control using random forests for building energy optimization and climate control. *Applied Energy*, 226, 1252-1272.
- Tang, R., & Wang, S. (2019). Model predictive control for thermal energy storage and thermal comfort optimization of building demand response in smart grids. *Applied Energy*, 242, 873-882.
- Tang, R., Wang, S., Gao, D.-c., & Shan, K. (2016). A power limiting control strategy based on adaptive utility function for fast demand response of buildings in smart grids. *Science and Technology for the Built Environment*, 22(6), 810-819.
- Tang, R., Wang, S., & Li, H. (2019). Game theory based interactive demand side management

- responding to dynamic pricing in price-based demand response of smart grids. *Applied Energy*, 250, 118-130.
- Tang, R., Wang, S., Shan, K., & Cheung, H. (2018). Optimal control strategy of central air-conditioning systems of buildings at morning start period for enhanced energy efficiency and peak demand limiting. *Energy*, 151, 771-781.
- Tang, R., Wang, S., & Yan, C. (2018). A direct load control strategy of centralized air-conditioning systems for building fast demand response to urgent requests of smart grids. *Automation in Construction*, 87, 74-83.
- Tuballa, M. L., & Abundo, M. L. (2016). A review of the development of Smart Grid technologies. *Renewable and Sustainable Energy Reviews*, 59, 710-725.
- Tuhus-Dubrow, D., & Krarti, M. (2010). Genetic-algorithm based approach to optimize building envelope design for residential buildings. *Building and Environment*, 45(7), 1574-1581.
- U.S. Department of Energy. 2011 DOE Building Energy Data Book. Available at: <http://buildingsdatabook.eren.doe.gov/>.
- Wang, J., Li, S., Chen, H., Yuan, Y., & Huang, Y. (2019). Data-driven model predictive control for building climate control: Three case studies on different buildings. *Building and Environment*, 160.
- Wang, S. (1998). Dynamic simulation of a building central chilling system and evaluation of EMCS on-line control strategies. *Building and Environment*, 33(1), 1-20.
- Wang, S., & Tang, R. (2017). Supply-based feedback control strategy of air-conditioning systems for direct load control of buildings responding to urgent requests of smart grids. *Applied Energy*, 201, 419-432.
- Xi, X.C., Poo, A.N., & Chou, S.K. (2007). Support vector regression model predictive control on a HVAC plant. *Control Engineering Practice*, 15(8), 897-908.
- Xu, L., Wang, S., & Tang, R. (2019). Probabilistic load forecasting for buildings considering weather forecasting uncertainty and uncertain peak load. *Applied Energy*, 237, 180-195.
- Xue, X., Wang, S., Yan, C., & Cui, B. (2015). A fast chiller power demand response control strategy for buildings connected to smart grid. *Applied Energy*, 137, 77-87.
- Yin, R., Xu, P., Piette, M. A., & Kiliccote, S. (2010). Study on Auto-DR and pre-cooling of commercial buildings with thermal mass in California. *Energy and Buildings*, 42(7), 967-975.
- Zhang, F., Deb, C., Lee, S. E., Yang, J., & Shah, K. W. (2016). Time series forecasting for building energy consumption using weighted Support Vector Regression with differential evolution optimization technique. *Energy and Buildings*, 126, 94-103.
- Zong, Y., Kullmann, D., Thavlov, A., Gehrke, O., & Bindner, H. W. (2012). Application of Model Predictive Control for Active Load Management in a Distributed Power System With High Wind Penetration. *IEEE Transactions on Smart Grid*, 3(2), 1055-1062.